THE JOURNAL OF PHYSICAL CHEMISTRY Letters

pubs.acs.org/JPCL

Site-Selective Reaction of Cl + Propene in Solid *para*-Hydrogen: Formation of 2-Chloropropyl Radicals

Jay C. Amicangelo[†,§] and Yuan-Pern Lee*[,†,‡]

[†]Department of Applied Chemistry and Institute of Molecular Science, National Chiao Tung University, 1001 Ta-Hsueh Road, Hsinchu 30010, Taiwan, and [‡]Institute of Atomic and Molecular Sciences, Academia Sinica, Taipei 10617, Taiwan

ABSTRACT The reaction of chlorine atoms with propene in a solid *para*-hydrogen matrix has been studied using infrared spectroscopy. For the Cl atom addition reaction, we find that the only observed isomer of the chloropropyl radical is the 2-chloropropyl and not the 1-chloropropyl radical, indicating that the addition of the Cl atom to the carbon−carbon double bond of propene occurs primarily at the central carbon atom. This is in sharp contrast to the generally accepted mechanism in organic chemistry and in gas-phase reactions in which the addition to the terminal carbon atom is greatly favored. This unique selectivity is possibly due to steric effects in solid *para*-hydrogen, in which the complex of Cl_2 and propene are positioned so that the reacting Cl atom is closer to the central versus the terminal carbon atom of propene. One might be able to make use of this unique property to perform selective chemistry.

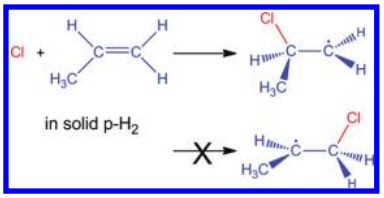

SECTION Kinetics, Spectroscopy

It has been suggested that the reactions of atomic chlorine with alkenes (C_nH_{2n}) may play an important role in various atmospheric processes, most notably in the chemistry of the Arctic troposphere.[1−3] These reactions have been studied in the gas phase both experimentally[4] and theoretically.[5−7] The two most significant initial processes are the addition of a Cl atom to the carbon−carbon double bond to form a chloroalkyl radical ($C_nH_{2n}Cl^{\bullet}$) or the abstraction of a hydrogen atom to form an alkyl radical ($C_nH_{2n-1}^{\bullet}$) and HCl; the branching ratio of these two reactions has been observed to depend on alkene structure, pressure, and temperature.[4] The two radical products then react further to give stable molecular products. On the basis of the resulting product distributions, a general rule has been established for the Cl atom addition reactions that the initial addition occurs primarily at the terminal or less substituted carbon of the alkene, giving rise to the radical product with lower energy; however, this selectivity is not exclusive for most alkenes, and addition at both sites is often observed.[4]

The simplest alkene in which the positional selectivity of the Cl addition reaction can be determined is propene (C_3H_6 or $CH_3CH{=}CH_2$). The reaction of Cl atoms with propene has been studied theoretically by Braña and Sordo using quantum chemical methods in order to understand the energetics and mechanism of the possible reaction products.[7] They predicted that the addition of the Cl atom to either carbon of the C=C bond is barrierless and exothermic and that both pathways proceed through a Cl atom−propene complex ($Cl{-}C_3H_6$) on the way to form the chloroalkyl radicals. The addition to the terminal carbon to form the 1-chloropropyl radical ($CH_3CH^{\bullet}CH_2Cl$) is predicted to be slightly lower in energy than the addition to the central carbon to form the 2-chloropropyl radical ($CH_3CHClCH_2^{\bullet}$) by 0.4 kJ/mol (see Figure 1 for structures). Therefore, on the basis of the predicted relative energies of the two addition pathways, quantum chemical calculations suggest that there should be very little preference for the addition of the Cl atom to the terminal versus the central carbon atom. Lee and Rowland experimentally studied the addition reactions of Cl atoms with propene at 293 K using thermal ^{38}Cl atoms and a radical scavenger (HI) to determine the site selectivity of these reactions.[8] In these experiments, the addition to the terminal carbon to form the 1-chloropropyl radical was found to be predominant over the addition to the central carbon to form the 2-chloropropyl radical with a ratio of 6.5−12.3 to 1, depending on the concentration of the scavenger.

Given the prominent role of chloroalkyl radicals in the mechanism of the reactions of chlorine atoms with alkenes, direct evidence of the existence of these species is important. Because of their short lifetimes under most conditions, no reports have been published in the literature on the experimental observation and spectral characterization of the chloropropyl radicals. In this regard, the matrix isolation infrared (IR) absorption technique has proven to be a valuable method to produce and spectrally characterize radicals and other unstable species.[9,10] The use of the matrix isolation technique with conventional matrixes (typically Ar or Ne) to study the reactions of Cl atoms with small molecules has been somewhat limited due to the cage effect in which the Cl atoms produced by ultraviolet (UV) irradiation of Cl_2 cannot escape

Received Date: August 9, 2010
Accepted Date: September 9, 2010
Published on Web Date: September 20, 2010

DOI: 10.1021/jz101119b | *J. Phys. Chem. Lett.* **2010**, *1*, 2956–2961

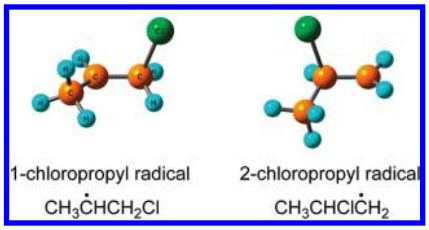

Figure 1. Minimum-energy structures of the 1-chloropropyl and 2-chloropropyl radicals calculated at the B3LYP/aug-cc-pVDZ level of theory.

the original matrix cage and therefore most of the products observed involve the reaction of both Cl atoms.[11,12] The use of solid *para*-hydrogen (*p*-H_2) as a matrix has generated considerable interest in recent years[13,14] because it is considered as a quantum solid due to the fact that the amplitude of the zero-point lattice vibrations is a large fraction of the lattice spacing.[15] Therefore, solid *p*-H_2 is "softer" than noble gas matrixes and this gives it several unique properties,[16−18] particularly a diminished cage effect,[19] which is relevant to the study of radical reactions, such as those of chlorine atoms with small molecules. Our group has recently demonstrated that codeposition of Cl_2 with CS_2 in *p*-H_2 followed by irradiation with UV light results in reaction products containing only a single chlorine atom, ClSCS, ClCS, and ClSC.[20]

In this Letter, we examined the reaction products resulting from the UV irradiation of codeposited Cl_2 and C_3H_6 in solid *p*-H_2 matrixes using IR spectroscopy. In these experiments, we have observed a series of IR bands that we have assigned to the 2-chloropropyl radical ($CH_3CHClCH_2^{\bullet}$) on the basis of comparison with vibrational frequencies calculated using density functional theory (DFT) and the behavior of the bands upon annealing and secondary photolysis. Interestingly, in sharp contrast to the reported gas-phase experimental results, it appears that the 2-chloropropyl radical is the primary observable single chlorine atom addition product in solid *p*-H_2 because we did not observe any bands that we can unambiguously assign to the 1-chloropropyl radical ($CH_3CH^{\bullet}CH_2Cl$).

The IR spectrum of C_3H_6 in *p*-H_2 at 3.2 K in the region between 500 and 1800 cm^{-1} exhibits a series of lines of varying intensity; the three largest are observed at 1651.4, 1455.8, and 912.1 cm^{-1}, in good agreement with the literature spectra of C_3H_6.[21,22] Upon codeposition of a mixture of Cl_2 with the C_3H_6 in *p*-H_2 at 3.2 K, several new distinct bands, as well as shoulders on many of the C_3H_6 bands, are observed, and we assign these bands to the $Cl_2{-}C_3H_6$ complex. These new bands are enhanced by approximately a factor of 3 upon gently annealing the matrix to 4.3 K, and the most prominent of these new bands are lines at 920.1 and 1455.2 cm^{-1}. To demonstrate this, two portions of the IR difference spectrum recorded upon annealing of the matrix to 4.3 K for 1 h after deposition of a $C_3H_6/Cl_2/p$-H_2 (1.0:1.3:2000) mixture at 3.2 K for 5 h are shown in Figure 2a. The lines pointing upward at 1045.0 and 587.2 cm^{-1} are due to the $Cl_2{-}C_3H_6$ complex, and the lines pointing downward at 1043.8 and 578.4 cm^{-1} are due to C_3H_6. The assignment of these new bands to that of the $Cl_2{-}C_3H_6$ complex was aided by DFT calculations, and the gas-phase structure of the $Cl_2{-}C_3H_6$ complex predicted at the

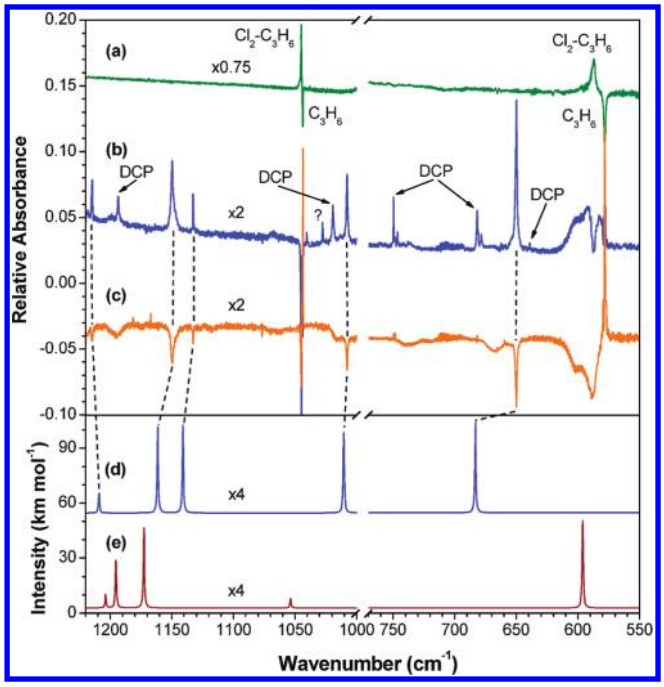

Figure 2. Experimental difference spectra (a−c) and simulated harmonic infrared spectra for the 2-chloropropyl (d) and 1-chloropropyl (e) radicals in the regions of 550−770 and 1000−1220 cm^{-1}. (a) Recorded at 3.2 K upon annealing of a $C_3H_6/Cl_2/p$-H_2 (1:1.3:2000) matrix to 4.3 K for 1 h after deposition for 5 h. The 4.3 K annealing was performed in this experiment in order to enhance the $Cl_2{-}C_3H_6$ complex bands. (b) Recorded at 3.2 K upon irradiation of a $C_3H_6/Cl_2/p$-H_2 (1:1:2000) matrix at 365 nm for 5 h after deposition for 10 h. Annealing to 4.3 K was not done in this experiment prior to 365 nm photolysis. (c) Recorded at 3.2 K upon irradiation of the matrix described in (b) at 254 nm for 4 h. Annealing of the matrix to 4.5 K for 50 min was done prior to 254 nm photolysis. For clarity, the difference spectra (a), (b), and (c) have been offset by approximately 0.14, 0.02, and −0.04 absorbance units, respectively. (d, e) Simulated spectra based on the unscaled harmonic frequencies of 2-chloropropyl and 1-chloropropyl radicals, respectively, computed at the B3LYP/aug-cc-pVDZ level of theory, with a simulated half-width of 0.5 cm^{-1} and a resolution of 0.25 cm^{-1}. The simulated spectra in (d) and (e) have been offset by approximately 55 and 3 km mol^{-1}, respectively, for clarity.

B3LYP/aug-cc-pVDZ level is shown in Figure 3 (left panels). Using the experimental intensities of the 1043.8 and the 1045.0 cm^{-1} bands in the original 4.3 K annealed spectrum and the corresponding theoretical IR intensities, we estimate that the ratio of the C_3H_6 to the $Cl_2{-}C_3H_6$ complex is approximately 12:1.

Upon photolysis of a deposited $C_3H_6/Cl_2/p$-H_2 mixture with 365 nm radiation for 5 h, a series of new infrared bands appear, which are generally reaction products between Cl atoms (produced via photodissociation of Cl_2) and C_3H_6, while the bands due to C_3H_6 and the $Cl_2{-}C_3H_6$ complex decrease in intensity. From an examination of the spectra before and after photolysis, we estimate that ∼4% of C_3H_6 and ∼60% of $Cl_2{-}C_3H_6$ were reacted during photolysis. The spectrum presented in Figure 2b is a difference spectrum obtained by subtracting the codeposited $C_3H_6/Cl_2/p$-H_2 spectrum from the spectrum after 5 h of irradiation at 365 nm. Several of the weak new bands shown in Figure 2b (678.6, 681.8, 746.6, 749.7, 1019.1, 1193.7, and

DOI: 10.1021/jz101119b | J. Phys. Chem. Lett. 2010, 1, 2956–2961

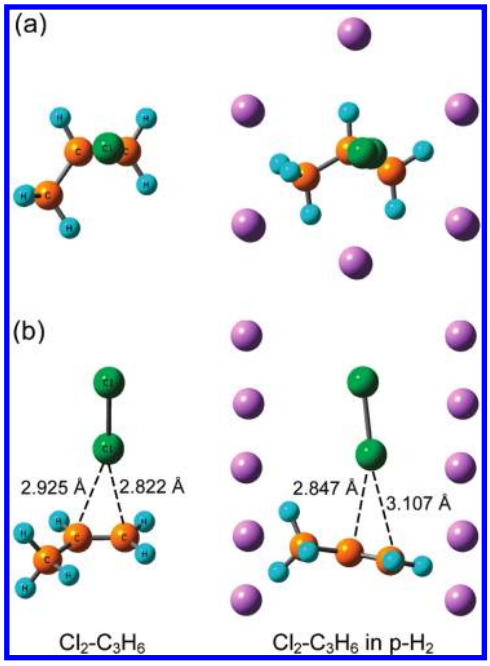

Figure 3. Minimum-energy structures of the $Cl_2-C_3H_6$ complex in the gas phase (left panels) and within a model hexagonal close-packed lattice of *para*-hydrogen (right panels) calculated at the B3LYP/aug-cc-pVDZ level of theory. Panel (a) is a view from the top of the complex looking down the Cl−Cl bond axis, and panel (b) is a side view obtained by rotating the structures approximately 90° from that displayed in (a). In the *para*-hydrogen model structure, the *para*-hydrogen molecules are being represented by single pink spheres, and some *para*-hydrogen molecules have been removed to reveal the structure of $Cl_2-C_3H_6$.

1236.7 cm^{-1}) are readily assigned to 1,2-dichloropropane, based on a comparison with the literature gas-phase spectrum[21] and a control experiment in which an authentic sample of 1,2-dichloropropane is deposited in a *p*-H_2 matrix at 3.2 K. In addition, weak bands of HCl and a $HCl-C_3H_6$ complex are observed in the 2700−2900 cm^{-1} region, and very weak bands that have been tentatively assigned to C_3H_5 and a $HCl-C_3H_5$ complex have also been observed near 800 and 980 cm^{-1}. Of the remaining new bands, the most prominent is a strong band at 649.9 cm^{-1}. In order to help determine the carriers of the remaining unassigned new bands, further experiments were performed, annealing to 4.5 K for 50 min (Figure S1, Supporting Information) followed by irradiation at 254 nm at 3.2 K for 4 h (Figure 2c).

Upon annealing the irradiated matrix, the bands due to C_3H_6 decreased in intensity, while those of the $Cl_2-C_3H_6$ complex increased slightly. Of the unassigned new bands observed with 365 nm irradiation, the band at 650 cm^{-1} was observed to increase slightly, indicating that this band is due to a reaction between Cl and C_3H_6 since some isolated Cl atoms would become mobile in the *p*-H_2 matrix at 4.5 K. In contrast to the 4.5 K annealing, when the matrix is subsequently photolyzed at 254 nm, the 650 cm^{-1} band exhibits a large decrease in intensity, Figure 2c. Along with the 650 cm^{-1} band, several other bands (1007.6, 1132.7, 1149.6, 1214.7, and 1382.2 cm^{-1}) are also observed to decrease at approximately the same rate and with nearly the same intensity ratio

Table 1. Comparison of Experimental Band Positions (cm^{-1}) and Relative Intensities Assigned to the 2-Chloropropyl Radical in *p*-H_2 with the Predicted Harmonic Vibrational Frequencies and Relative Intensities Calculated at the B3LYP/aug-cc-pVDZ Level

mode description	ν_{expt}	I_{expt}[a]	ν_{DFT}	I_{DFT}[a]
CH_3 deformation	1382.2	16	1397	18
β-CH out-of-plane bend	1214.7	10	1209	5
β-CH in-plane bend	1149.6	31	1161	22
β-CH out-of-plane bend	1132.7	6	1140	22
CH_3 rocking	1007.6	19	1010	21
CH_2 out-of-plane bend	649.9	100	683	100

[a] Intensities are normalized to the most intense band. Experimental IR intensities are estimated by integrating the areas of the corresponding bands. The B3LYP/aug-cc-pVDZ predicted intensity for the 683 cm^{-1} band is 53.0 km mol^{-1}.

to the 650 cm^{-1} band as was observed in the spectrum in Figure 2b. This suggests that these bands all belong to a common species. When the peak pattern of these bands in Figure 2b and c are compared with the DFT predicted vibrational spectra for the 1-chloropropyl and the 2-chloropropyl radical in Figure 2e and d, respectively, it is clear that the best agreement is with the 2-chloropropyl radical. Therefore, we assign these bands to the 2-chloropropyl radical (Table 1). As described in the Experimental and Computational Methods section, the 365 nm photolysis experiments have been performed both with and without prior 4.3 K annealing, and the bands that have been assigned to the 2-chloropropyl radical are observed in all experiments with the same relative intensities. The only differences observed for these bands in the various experiments is with the absolute intensities of the bands, which seem to track with the absolute intensities of the $Cl_2-C_3H_6$ complex bands regardless of the thermal history of the matrix.

Having assigned the bands listed in Table 1 to the 2-chloropropyl radical, we examined the spectra carefully to determine if any additional bands in the spectra can be assigned unambiguously to the 1-chloropropyl radical. There is a set of broad of features near 600 cm^{-1} in the difference spectra presented in Figure 2b and c that appear to match the most intense predicted band of the 1-chloropropyl radical. However, close inspection of the original spectra indicates that these bands are a result of changes in the intensities of the large peaks of C_3H_6 and $Cl_2-C_3H_6$ at 578.4 and 587.2 cm^{-1}, respectively, and a small change in the intensity of the background just higher than 600 cm^{-1}. Therefore, we cannot assign any feature in this region to a band of the 1-chloropropyl radical with any confidence nor are we able to unambiguously assign any other observed band in the spectra to the 1-chloropropyl radical. Using a detection limit for the absorbance difference of 0.006 and theoretically predicted IR intensities of the most prominent bands of the 1-chloropropyl and 2-chloropropyl radicals, we conclude that when chlorine atoms react with propene in a solid *p*-H_2 matrix, the addition of the Cl atom occurs at the central carbon to form the 2-chloropropyl radical ($CH_3CHClCH_2^{\bullet}$) at least 20 times more effectively than that at the terminal carbon to form the 1-chloropropyl radical ($CH_3CH^{\bullet}CH_2Cl$).

DOI: 10.1021/jz101119b | J. Phys. Chem. Lett. 2010, 1, 2956–2961

This result is significant and noteworthy for two reasons. First, the fact that we can observe and characterize a radical reaction product containing only one Cl atom is further illustration of the diminished cage effect in solid *p*-H_2, allowing one of the Cl atoms to escape the matrix cage after the photodissociation of Cl_2. This feature allows us to produce a chloropropyl radical and spectrally characterize it for the first time. Second, the observation of only the 2-chloropropyl radical when the reaction of Cl with C_3H_6 is performed in a *p*-H_2 matrix is significant because of the fact that when the reaction is performed in the gas phase,[8] the formation of the 1-chloropropyl radical is actually favored over the 2-chloropropyl radical by at least six times. As well, high-level quantum chemical calculations on the reaction Cl + C_3H_6 predict that the addition of the Cl atom to either carbon is barrierless and that formation of the 1-chloropropyl radical is energetically favored by only 0.4 kJ/mol over formation of the 2-chloropropyl radical,[7] which would suggest very little preference for the addition of the Cl atom to the terminal versus the central carbon atom.

One possible explanation of this unique selectivity in *p*-H_2 could be size restrictions and steric effects within the solid *p*-H_2 matrix that cause the reacting Cl atom to be guided to the central carbon atom rather than the terminal carbon of C_3H_6. The observation that the Cl_2−C_3H_6 complex bands decrease substantially with 365 nm irradiation suggests that a large portion of the 2-chloropropyl radical is being formed from the Cl_2−C_3H_6 complex as a precursor following photodissociation of the Cl_2. Therefore, the geometry of the Cl_2−C_3H_6 complex within the solid *p*-H_2 matrix might have an effect on the reactivity between Cl and C_3H_6. With this in mind, we have performed additional DFT calculations in which the geometry of the Cl_2−C_3H_6 complex is optimized within a model of solid *p*-H_2 in an attempt to help understand our observation of only the 2-chloropropyl radical.

At 3.2 K, the thermodynamically most stable phase of solid *p*-H_2 is the hexagonal close-packed (hcp) crystal structure, and within a single hcp layer, each *p*-H_2 molecule is separated by 3.76 Å.[23] Due to the large sizes of C_3H_6 and Cl_2, when modeling the Cl_2−C_3H_6 complex within a hcp lattice of *p*-H_2, we have chosen to use three adjacent substitutional sites located along the *a* axis within a single *p*-H_2 hcp layer as the space available to the Cl_2−C_3H_6 complex. For the initial geometry of the Cl_2−C_3H_6 complex, the optimized gas-phase structure obtained at the B3LYP/aug-cc-pVDZ level (Figure 3, left panels) was used, and this structure was placed within the vacant sites in the *p*-H_2 lattice. The orientation of the Cl_2−C_3H_6 complex was such that the carbon−carbon double bond was parallel to the *bc* plane of the hcp lattice, which then positioned the Cl_2 nearly parallel to the *a* axis. The geometry of the Cl_2−C_3H_6 complex was then optimized within the *p*-H_2 hcp lattice at the B3LYP/aug-cc-pVDZ level while holding the *p*-H_2 lattice fixed during the optimization. The structure that resulted from this optimization is displayed in the right panels of Figure 3.

As can be seen in Figure 3, the constraints of the *p*-H_2 lattice produce substantial changes in the geometry of the Cl_2−C_3H_6 complex. Whereas in the gas phase the Cl_2 is approximately perpendicular to the plane of the C═C bond in C_3H_6, in the *p*-H_2 lattice, the Cl_2 and the C═C bond plane of C_3H_6 are tilted slightly with respect to the *p*-H_2 layers. This is most likely due to steric interactions between the Cl_2−C_3H_6 and the *p*-H_2 lattice, and the tilting of Cl_2 and C_3H_6 within the substitutional sites relieves these repulsive interactions. There are also significant changes to the distances between the reacting chlorine atom (the one adjacent to the C_3H_6) and the alkene carbon atoms. In the gas phase, the distances between this Cl atom and the terminal and central carbon atoms are predicted to be 2.822 and 2.925 Å, respectively, whereas in the *p*-H_2 lattice, the analogous distances are predicted to be 3.107 and 2.847 Å, respectively.

Thus, the calculations suggest that in a *p*-H_2 lattice, the reacting Cl atom will be much closer to the central carbon atom than the terminal carbon atom, as opposed to the gas phase in which the Cl atom is closer to the terminal carbon. From a simplistic viewpoint of energetics, this shortening of the distance between the Cl atom and the central carbon would likely lead to an energy lowering of the reaction path toward the central carbon versus the pathway toward the terminal carbon. Also, given the position of the terminal carbon toward the edge of the *p*-H_2 cage in the right panels of Figure 3 and the van der Waals diameter of a Cl atom (~3.6 Å[24]), it seems reasonable to assume that the Cl atom might experience repulsive interactions upon approach and attachment at the terminal carbon in *p*-H_2. Therefore, once the reaction is initiated by the photodissociation of the Cl_2, it would be less likely that the reacting Cl atom would deviate out of the minimum-energy pathway toward the central carbon to attack the terminal carbon. This could then lead to an increased probability of formation of the 2-chloropropyl radical. In a way, one could say that the *p*-H_2 lattice is guiding the Cl atom to the central carbon atom because it influences the potential energy surface of the reaction in that specific direction by altering part of the reaction entrance channel, which in this case might be the Cl_2−C_3H_6 complex geometry. This is a very exciting prospect in that it suggests that with judicious choice of reacting partners, a Cl atom could possibly be directed to a very specific and desired reaction site in a *p*-H_2 matrix.

We cannot positively exclude the possibility that the observed selectivity might be influenced by the selectivity of secondary reactions of Cl adding to the chloropropyl radicals. However, using calculated IR intensities for both the 2-chloropropyl radical and 1,2-dichloropropane, we estimate that the relative yield of the 2-chloropropyl radical to 1,2-dichloropropane ranges from 3.5 to 7.2, depending on the peaks used in the calculation and on the concentration of Cl_2. This indicates that even if all of the 1-chloropropyl radical were to react with Cl to form 1,2-dichloropropane, the preferential formation of the 2-chloropropyl radical is still significant.

Overall, the work presented in this report clearly demonstrates the unique nature of low-temperature solid *p*-H_2 matrixes as a reaction medium. It is a soft matrix in that it exhibits a diminished cage effect to allow for the reaction between a single Cl atom and C_3H_6 to form a monochloropropyl radical rather than merely dichloropropane. Furthermore and more importantly, the sole Cl atom addition product that we observe is the 2-chloropropyl radical, which is

DOI: 10.1021/jz101119b | J. Phys. Chem. Lett. 2010, 1, 2956–2961

considerably different from what is generally accepted in chlorine solution chemistry and in the gas-phase reaction. The site selectivity mediated by the *p*-H_2 matrix resembles that observed in some biological systems and might lead to significant applications in the future.

EXPERIMENTAL AND COMPUTATIONAL METHODS

The details of the matrix isolation apparatus used in these experiments have been described previously.[18,20,25] In these experiments, separate mixtures of C_3H_6 (99.5%, AGA, used as received) and Cl_2 (99.9%, Air Products and Chemicals, used as received) in *para*-hydrogen (produced as described below) were codeposited simultaneously onto a gold-plated copper block, which also served as a mirror to reflect the incident infrared beam to the detector, at 3.2 K (achieved with a Janis RDK-415 closed-cycle helium cryostat system) for 5−10 h at equal rates of 7−8 mmol/hour. The concentration of the Cl_2/*p*-H_2 mixture was between 1:800 and 1:1000, and the concentration of the C_3H_6/*p*-H_2 mixture was 1:1000. *p*-H_2 was produced by a low-temperature conversion process in which normal H_2 gas (99.9999%, Scott Specialty Gases) is passed through a copper coil filled with a hydrated iron(III) oxide catalyst (catalyst grade, 30−50 mesh, Sigma-Aldrich) that is cooled with a closed-cycle helium refrigerator (Advanced Research Systems, DE204AF). The efficiency of the conversion is controlled by the temperature of the catalyst, which was typically 13−15 K in these experiments. At these temperatures, the concentration of *ortho*-hydrogen is less than 100 ppm according to the Boltzmann distribution. Prior to entering the catalyst coil, the H_2 gas was passed through a trap cooled to 77 K before conversion to *p*-H_2. Infrared absorption spectra were recorded with a Bomem DA8 Fourier-transform infrared spectrometer (FTIR) equipped with a KBr beamsplitter and a Hg/Cd/Te detector cooled to 77 K to cover the spectral range of 500−5000 cm^{-1}. Typically, 400 scans at 0.25 cm^{-1} resolution were coadded at each stage of the experiment.

After the initial codeposition of the Cl_2/*p*-H_2 and C_3H_6/*p*-H_2 mixtures, some of the deposited matrixes were then annealed at 4.3 K for up to 1 h to enhance the production of the intermolecular complex between Cl_2 and C_3H_6, denoted as Cl_2−C_3H_6. To produce Cl atoms for reaction with C_3H_6, the C_3H_6/Cl_2/*p*-H_2 matrixes were irradiated with 365 nm radiation from a light-emitting diode (Honle UV Technology, 375 mW) for 2−5 h. It has been previously reported that infrared excitation of the solid *p*-H_2 bands (4000−5000 cm^{-1}) can induce Cl atoms to react with *p*-H_2 to form HCl,[26] and therefore, when Cl atoms were present in the *p*-H_2 matrix, a 2.4 μm infrared cutoff filter (Andover Corp.) was used when recording the infrared spectra. Following the photolysis at 365 nm, the matrix was sometimes annealed to 4.5 K to induce further reaction, and for all matrixes, secondary photolysis was performed using a low-pressure Hg lamp (Pen-Ray lamp, UVP) with a 254 nm band-pass filter (ESCO Products) to help distinguish the related product bands in the spectra.

Quantum chemical calculations were used to aid in the identification and interpretation of the spectra obtained. In this work, density functional theory calculations using the B3LYP hybrid functional[27−29] and the aug-cc-pVDZ basis set[30] were performed to predict equilibrium geometries and vibrational frequencies of the possible species that might be observed in these experiments. All calculations used the Gaussian 03 suite of programs.[31]

SUPPORTING INFORMATION AVAILABLE The 4.5 K annealed spectrum (Figure S1) and coordinates and energies of DFT optimized structures (Table S1). This material is available free of charge via the Internet at http://pubs.acs.org.

AUTHOR INFORMATION

Corresponding Author:

*To whom correspondence should be addressed. Phone: (886)-3-5131459. E-mail: yplee@mail.nctu.edu.tw. Fax: (886)-3-5713491.

Notes

§ On sabbatical leave from School of Science, Penn State Erie, The Behrend College, 4205 College Drive, Erie, PA 16563.

ACKNOWLEDGMENT This work was supported by the National Science Council of Taiwan Grant NSC98-2113-M-009-001-ASP. J.A. also acknowledges support in the form of a Fulbright Research Grant from the Foundation for Scholarly Exchange (Fulbright Taiwan) and the J. William Fulbright Foreign Scholarship Board (U.S. State Department). The National Center for High-Performance Computing of Taiwan provided computer time for some of the DFT calculations.

REFERENCES

(1) Finlayson-Pitts, B. J.; Pitts, J. N., Jr. *Chemistry of the Upper and Lower Atmosphere*; Academic: San Diego, CA, 2000.
(2) Kiel, A. D.; Shepson, P. B. Chlorine and Bromine Atom Ratios in the Springtime Artic Troposphere as Determined from Measurements of Halogenated Volatile Organic Compounds. *J. Geophys. Res.* **2006,** *111*, D17303.
(3) Tackett, P. J.; Cavender, A. E.; Kiel, A. D.; Shepson, P. B.; Bottenheim, J. W.; Morin, S.; Deary, J.; Steffen, A.; Doerge, C. A Study of the Vertical Scale of Halogen Chemistry in the Artic Troposphere During Polar Sunrise at Barrow, Alaska. *J. Geophys. Res.* **2007,** *112*, D07306.
(4) Taatjes, C. A. Time-Resolved Infrared Absorption Measurements of Product Formation in Cl Atom Reactions with Alkenes and Alkynes. *Int. Rev. Phys. Chem.* **1999,** *18*, 419–458.
(5) Brana, P.; Menendez, B.; Fernandez, T.; Sordo, J. A. Potential Energy Surface for the Chlorine Atom Reaction with Ethylene: A Theoretical Study. *J. Phys. Chem. A* **2000,** *104*, 10842–10854.
(6) Brana, P.; Sordo, J. A. Mechanistic Aspects of the Abstraction of an Allylic Hydrogen in the Chlorine Atom Reaction with 2-Methyl-1,3-Butadiene (Isoprene). *J. Am. Chem. Soc.* **2001,** *123*, 10348–10353.
(7) Brana, P.; Sordo, J. A. Theoretical Approach to the Mechanism of the Reactions Between Halogen Atoms and Unsaturated Hydrocarbons: The Cl + Propene Reaction. *J. Comput. Chem.* **2003,** *24*, 2044–2062.
(8) Lee, F. S. C.; Rowland, F. S. Thermal Chlorine-38 Reactions with Propene. *J. Phys. Chem.* **1977,** *81*, 1222–1229.
(9) Hallam, H. E., Ed. *Vibrational Spectroscopy of Trapped Species*; Wiley: New York, 1973.

DOI: 10.1021/jz101119b | *J. Phys. Chem. Lett.* **2010,** *1*, 2956–2961

(10) Andrews, L.; Moskovits, M., Eds. *Chemistry and Physics of Matrix-Isolated Species*; North-Holland: Amsterdam, The Netherlands, 1989.
(11) Tobin, Y. A.; Nieto, L. I.; Romano, R. M.; Della Vedova, C. O.; Downs, A. J. Photochemical Reaction Channels of OCS with Cl_2, ICl, or IBr Isolated Together in an Argon Matrix: Isolation of *syn*-Iodocarbonylsulfenyl Bromide. *J. Phys. Chem. A* **2006,** *110*, 2674–2681.
(12) Tobin, Y. A.; Romano, R. M.; Della Vedova, C. O.; Downs, A. J. Formation of New Halogenothiocarbonylsulfenyl Halides, XC(S)SY, Through Photochemical Matrix Reactions Starting from CS_2 and a Dihalogen Molecule XY (XY = Cl_2, Br_2, or BrCl). *Inorg. Chem.* **2007,** *46*, 4692–4703.
(13) Momose, T.; Shida, T. Matrix-Isolation Spectroscopy Using Solid Parahydrogen as the Matrix: Application to High-Resolution Spectroscopy, Photochemistry, and Cryochemistry. *Bull. Chem. Soc. Jpn.* **1998,** *71*, 1–15.
(14) Yoshioka, K.; Raston, P. L.; Anderson, D. T. Infrared Spectroscopy of Chemically Doped Solid Parahydrogen. *Int. Rev. Phys. Chem.* **2006,** *25*, 469–496.
(15) Van Kranendonk, J. *Solid Hydrogen: Theory of the Properties of Solid H2, HD, and D2*; Plenum: New York, 1983.
(16) Tam, S.; Fajardo, M. E.; Katsuki, H.; Wakabayashi, T.; Momose, T. High Resolution Infrared Absorption Spectra of Methane Molecules Isolated in Solid Parahydrogen Matrices. *J. Chem. Phys.* **1999,** *111*, 4191–4198.
(17) Momose, T.; Hoshina, H.; Fushitani, M.; Katsuki, H. High-Resolution Spectroscopy and the Analysis of Ro-Vibrational Transitions of Molecules in Solid Parahydrogen. *Vib. Spectrosc.* **2004,** *34*, 95–108.
(18) Lee, Y.-P.; Wu, Y.-J.; Lees, R. M.; Xu, L.-H.; Hougen, J. T. Internal Rotation and Spin Conversion of CH_3OH in Solid Para-Hydrogen. *Science* **2006,** *311*, 365–368.
(19) Wu, Y.-J.; Yang, X.; Lee, Y.-P. Infrared Matrix Isolation Spectroscopy Using Pulsed Deposition of *p*-H_2. *J. Chem. Phys.* **2004,** *120*, 1168–1171.
(20) Huang, C.-W.; Lee, Y.-C.; Lee, Y.-P. Diminished Cage Effect in Solid *p*-H_2: Infrared Spectra of ClSCS, ClCS, and ClCS in an Irradiated *p*-H_2 Matrix Containing Cl_2 and CS_2. *J. Chem. Phys.* **2010,** *132*, 164303.
(21) Linstrom, P. J.; Mallard, W. G., Eds. *NIST Chemistry WebBook*, NIST Standard Reference Database Number 69; National Institute of Standards and Technology: Gaithersburg, MD. http://webbook.nist.gov (accessed April 2, 2010 and May 12, 2010).
(22) Coleman, W. M., III; Gordon, B. M. Examinations of the Matrix Isolation Fourier Transform Infrared Spectra of Organic Compounds: Part IX. *Appl. Spectrosc.* **1988,** *42*, 666–670.
(23) Mills, R. L.; Schuch, A. F. On the Crystal Structure of Normal Hydrogen at Low Temperature. *Phys. Rev. Lett.* **1965,** *15*, 722–724.
(24) Batsanov, S. S. Van der Waals Radii of Elements. *Inorg. Mater.* **2001,** *37*, 871–885.
(25) Lee, Y.-P.; Wu, Y.-J.; Hougen, J. T. Direct Spectral Evidence of Single-Axis Rotation and *ortho*-Hydrogen Assisted Nuclear Spin Conversion of CH_3F in Solid *para*-Hydrogen. *J. Chem. Phys.* **2008,** *129*, 104502.
(26) Raston, P. L.; Anderson, D. T. Infrared-Induced Reaction of Cl Atoms Trapped in Solid Parahydrogen. *Phys. Chem. Chem. Phys.* **2006,** *8*, 3124–3129.
(27) Becke, A. D. Density-Functional Exchange-Energy Approximation with Correct Asymptotic Behavior. *Phys. Rev. A* **1988,** *38*, 3098–3100.
(28) Becke, A. D. Density-Functional Thermochemistry. IV. A New Dynamical Correlation Functional and Implications for Exact-Exchange Mixing. *J. Chem. Phys.* **1996,** *104*, 1040–1046.
(29) Lee, C.; Yang, W.; Parr, R. G. Development of the Colle-Salvetti Correlation-Energy Formula into a Functional of the Electron Density. *Phys. Rev. B* **1988,** *37*, 785–789.
(30) Kendall, R. A.; Dunning, T. H., Jr.; Harrison, R. J. Electron Affinities of the First-Row Atoms Revisited. Systematic Basis Sets and Wave Functions. *J. Chem. Phys.* **1992,** *96*, 6796–6806.
(31) Frisch, M. J.; Trucks, G. W.; Schlegel, H. B.; Scuseria, G. E.; Robb, M. A.; Cheeseman, J. R.; Montgomery, J. A.; Vreven, T.; Kudin, K. N.; Burant, J. C.; et al. *Gaussian 03*, revision D.01; Gaussian, Inc.: Wallingford, CT, 2004.

DOI: 10.1021/jz101119b | *J. Phys. Chem. Lett.* **2010,** *1*, 2956–2961